



Published in final edited form as:

Nature. 2009 July 23; 460(7254): 534–537. doi:10.1038/nature08111.

The CREB Coactivator CRTC2 Links Hepatic ER Stress and Fasting Gluconeogenesis

Yiguo Wang, Liliana Vera, Wolfgang H. Fischer, and Marc Montminy

Clayton Foundation Laboratories for Peptide Biology, The Salk Institute for Biological Studies, 10010 N. Torrey Pines Rd., La Jolla CA, 92037

Abstract

In fasted mammals, circulating pancreatic glucagon stimulates hepatic gluconeogenesis in part through the CREB Regulated Transcription Coactivator 2 (CRTC2; also referred to as TORC2) 1,2. Hepatic glucose production is elevated in obesity, reflecting chronic increases in endoplasmic reticulum (ER) stress that promote insulin resistance 3. Whether ER stress also modulates the gluconeogenic program directly, however, is unclear. Here we show that CRTC2 functions as a dual sensor for ER stress and fasting signals in liver. Acute increases in ER stress triggered the dephosphorylation and nuclear entry of CRTC2, which in turn promoted the expression of ER quality control genes through an association with Activating Transcription Factor 6 alpha (ATF6 α), an integral branch of the unfolded protein response 4–9. In addition to mediating CRTC2 recruitment to ER stress inducible promoters, ATF6 α also reduced hepatic glucose output by disrupting the CREB:CRTC2 interaction and thereby inhibiting CRTC2 occupancy over gluconeogenic genes. Conversely, hepatic glucose output was upregulated when hepatic ATF6 α protein amounts were reduced, either by RNAi-mediated knockdown or as a result of persistent stress in obesity. As ATF6 α over-expression in livers of obese mice reversed CRTC2 effects on the gluconeogenic program and lowered hepatic glucose output, our results demonstrate how cross-talk between ER stress and fasting pathways at the level of a transcriptional coactivator contributes to glucose homeostasis.

Obesity is a central risk factor in the development of insulin resistance, which is characterized by an inability for insulin to inhibit glucose output from the liver and to increase glucose uptake into skeletal muscle 10,11. Although the underlying mechanism is unclear, obesity has been found to disrupt insulin signaling in liver and adipose through chronic increases in endoplasmic reticulum stress 3. Because hepatic glucose production is also increased in obesity, we investigated whether ER stress signals modulate the gluconeogenic program directly.

Users may view, print, copy, and download text and data-mine the content in such documents, for the purposes of academic research, subject always to the full Conditions of use:http://www.nature.com/authors/editorial_policies/license.html#terms

Corresponding Author: Marc Montminy MD., Ph.D., The Salk Institute, Phone: 858-453-4100, e-mail: montminy@salk.edu.

Author Contributions: YW and LV performed in vivo imaging studies; YW performed in vitro and biochemical studies; WF carried out mass spectrometry analysis. YW and MM designed the study, analyzed the data, and wrote the paper. All authors reviewed and commented on the manuscript.

Previous studies showing an important role for the CREB coactivator CRTC2 in promoting hepatic gluconeogenesis 1,2 led us to examine effects of ER stress in this setting. Exposure of primary hepatocytes to the ER stress activators thapsigargin (THA) or tunicamycin (TUN) 6 stimulated CRTC2 dephosphorylation and nuclear entry (fig. 1a,b; sup. fig. 1); these effects were blocked when cells were pre-treated with cyclosporine, an inhibitor of the Ser/Thr phosphatase calcineurin/PP2B, which has been shown to mediate CRTC2 dephosphorylation 12,13.

We used an adenovirally encoded cAMP responsive (Ad-CRE luc) reporter to monitor CREB:CRTC2 activity in primary hepatocytes. Although they stimulated an ER stress-inducible reporter (X Box Binding Protein 1 (Xbp1)-luc) 7,14, THA and TUN inhibited Ad-CRE luc activity, even when cells were co-stimulated with the cAMP activator forskolin (FSK; fig. 1a, bottom).

Having seen that ER stress promotes CRTC2 activation but not CREB-dependent transcription, we considered the potential involvement of a CRTC2 inhibitor in this process. In proteomic studies to identify cellular proteins that associate with CRTC2, we recovered the basic leucine zipper (bZIP) transcription factor ATF6 α from immunoprecipitates of endogenous CRTC2 (sup. fig. 2a). We confirmed the CRTC2: ATF6 α interaction in co-immunoprecipitation studies of primary hepatocytes using endogenous and epitope-tagged proteins (fig. 1c; sup. fig. 2a).

Localized to the ER under basal conditions, ATF6 α undergoes intramembrane proteolysis and nuclear shuttling in response to ER stress, when it promotes cell viability by stimulating ER quality control gene expression 4–9. CRTC2 was found to interact with the transcriptionally active cytoplasmic N-terminal (ATF6 N; aa 1–381) domain but not with the ER luminal C-terminal domain of ATF6 α (ATF6 C; aa. 382–670) (fig. 1d). Conversely, ATF6 α associated with an N-terminal CRTC2 polypeptide (aa. 1–120) that also mediates an interaction with CREB (sup. fig. 2b) 15,16.

We examined effects of ER stress on the recruitment of CRTC2 to ATF6 α -regulated genes. Under basal conditions, about one-third of cellular CRTC2 was localized to the cytoplasmic surface of the ER (sup. fig. 3). Following exposure of primary hepatocytes to THA or TUN, ATF6 α and CRTC2 shuttled to the nucleus where they occupied the Xbp1 promoter 7 (fig. 2a, top). ATF6 α over-expression augmented CRTC2 occupancy, while RNAi-mediated knockdown of ATF6 α blocked it (fig. 2a, bottom). And CRTC2 over-expression increased Ad-Xbp1 luc reporter activity whereas RNAi-mediated depletion of CRTC2 reduced it (fig. 2b). Consistent with a requirement for ATF6 α , CRTC2 did not up-regulate Ad-Xbp1 luc activity when cells were depleted of ATF6 α .

During *ad libitum* feeding, CRTC2 activity is silenced through phosphorylation at Ser171 by Salt Inducible Ser/Thr Kinase 2 (SIK2); these effects are reversed during fasting, when glucagon inhibits SIK2 activity via protein kinase A (PKA)-mediated phosphorylation 1. Pointing to a role for this kinase in the ER stress response, SIK2 over-expression disrupted Ad-Xbp1 luc reporter activity in ER-stressed hepatocytes, while RNAi-mediated knockdown augmented it (sup. fig. 4a, b). Conversely, over-expression of phosphorylation-

defective, active S171A mutant CRTC2 increased Ad-Xbp1 luc reporter activity constitutively in cells co-expressing active ATF6N (sup. fig. 4c).

We examined whether CRTC2 modulates hepatic ER stress responses *in vivo*. Triggering of the ER stress pathway by intraperitoneal (IP) injection of TUN increased Ad-Xbp1 luc reporter activity and ER stress gene expression in both fasted and *ad libitum* fed mice (fig. 2c; Xbp1, GRP78, and CHOP; sup. figs. 4d, 5, 6); these effects were attenuated by RNAi-mediated depletion of hepatic ATF6 α (sup. fig. 7). Similar to its effects in hepatocytes, Ad-CRTC2 expression also enhanced hepatic Ad-Xbp1 luc reporter activity and ER stress gene expression in TUN-injected mice, while RNAi-mediated depletion of CRTC2 down-regulated it (fig. 2c, d; sup. fig. 8). Taken together, these results indicate that CRTC2 promotes the expression of ER quality control genes in liver via an association with ATF6 α .

We considered that ATF6 α could interfere with induction of the gluconeogenic program through the CREB:CRTC2 pathway should cellular levels of CRTC2 be limiting. Supporting this idea, exposure of primary hepatocytes to THA or TUN increased the binding of ATF6 α (p50) to CRTC2 and reciprocally reduced amounts of CRTC2 associated with CREB (fig. 3a, top). Over-expression of nuclear, active ATF6N also decreased the CREB:CRTC2 interaction, and it blocked recruitment of CRTC2 to the gluconeogenic G6Pase promoter in FSK-treated cells (fig. 3a; sup. fig. 9). ATF6N expression also decreased Ad-CRE luc reporter activity, gluconeogenic gene expression, and glucose output from primary hepatocytes, while RNAi-mediated depletion of ATF6 α increased it (fig. 3b; sup. fig. 9). Confirming the importance of the ATF6 α :CRTC2 interaction, a mutant (Arg337Ala) ATF6 α polypeptide with lower affinity for CRTC2 was less potent in disrupting CREB activity relative to wild-type (sup. fig. 10).

Because ATF6 α and CREB bind to the same domain in CRTC2, CREB may reciprocally down-regulate ATF6 α activity. Indeed, Ad-CREB expression not only reduced Ad-Xbp1 luc reporter activity, but it also increased CRE-luc reporter activity and glucose production in hepatocytes expressing ATF6N (fig. 3b, sup. fig. 11). Taken together, these results indicate that CREB and ATF6 α exert counter-regulatory effects on gluconeogenesis, in part by competing for CRTC2 .

We tested the role of ATF6 α in modulating glucose balance *in vivo*. Modest hepatic over-expression of ATF6 α lowered the fasting gluconeogenic profile - which consists of hepatic Ad-CRE luc activity, gluconeogenic gene expression, and circulating blood glucose concentrations - in control mice, and to a greater extent in mice injected IP with TUN (fig. 3c; sup. fig. 12a). By contrast, RNAi-mediated depletion of hepatic ATF6 α increased the fasting gluconeogenic profile in both control and TUN-injected animals (fig. 3d; sup. fig. 12b).

Considering that ER stress is chronically upregulated in obesity 3 and that ATF6 α undergoes proteasome-dependent degradation when ER stress is prolonged 8, we tested whether hepatic ATF6 α activity is altered in this setting. Relative to lean controls, obese (*ob/ob*, *db/db*) mice exhibited lower Ad-Xbp1 luc reporter activities, and they had reduced hepatic ATF6 α protein amounts (fig. 4a; sup. fig. 13). By contrast, Ad-CRE luc activity,

gluconeogenic gene expression, and circulating blood glucose concentrations were all elevated in both *ob/ob* and *db/db* animals.

Because RNAi-mediated depletion of ATF6 α increases CRE-luc activity and hepatic glucose output, we wondered whether the obesity-related loss of hepatic ATF6 α would have similar effects on CREB and CRTC2. In that case, ATF6 α over-expression should improve glucose balance by lowering gluconeogenic gene expression. Supporting this notion, adenoviral expression of active ATF6N reduced fasting hepatic Ad-CRE luc activity as well as mRNA amounts for gluconeogenic genes in both *db/db* and high fat diet-fed (DIO) mice (fig. 4b, c; sup. fig. 14). Over-expression of ATF6N also lowered circulating blood glucose levels and enhanced glucose tolerance (fig. 4b, c; sup. fig. 15). Arguing against a significant effect of ATF6N on insulin signaling per se, hepatic amounts for inactive phospho (Ser307) Insulin Receptor Substrate 1 (IRS1) or active phospho-(Thr308) AKT appeared comparable between ATF6N-expressing and control mice (sup. fig. 15).

Taken together, these results indicate that CRTC2 functions as a dual sensor for fasting and ER stress signals (sup. fig. 16). The attendant cross-talk between these pathways appears to protect against excessive increases in hepatic gluconeogenesis that otherwise lead to chronic hyperglycemia in obesity. In addition to its effects on ATF6 α , chronic ER stress has also been found to increase hepatic gluconeogenesis and lipogenesis by triggering other branches of the unfolded protein response 17. Future studies should reveal the extent to which these pathways promote glucose intolerance through CREB or other bZIP transcription factors.

METHODS SUMMARY

Adenoviruses were delivered to 8–10 week old male mice by tail vein injection. Mice expressing CRE-luc or Xbp1-luc reporters were imaged on an IVIS 100 Imaging System under ad libitum feeding conditions or after fasting 1. Hepatic ER stress was induced in vivo by intraperitoneal (IP) injection of tunicamycin 6; effects of TUN on reporter activity and hepatic gene expression were evaluated 10 hours following TUN administration. For glucose tolerance tests, mice were fasted overnight and then injected IP with glucose. Effects of ER stress on glucose output, luciferase reporter activity, and gluconeogenic gene expression were also examined using primary hepatocyte cultures 12. Relative occupancy of ATF6, CREB, and TORC2 over relevant promoters in hepatocytes was determined by chromatin immunoprecipitation (ChIP) assay 2. CRTC2-associated proteins were identified using immunoprecipitates of endogenous and epitope-tagged CRTC2 prepared from HEK293T cells 12 and analyzed by electrospray ionization tandem mass spectrometry.

METHODS

Mouse strains and adenovirus

Adenoviruses (1×10^8 plaque forming units (pfu) CRTC2 RNAi, CRTC2, ATF6 α RNAi, ATF6 α , ATF6N (1–381), or unspecific RNAi, 10^9 pfu CRE-luc or Xbp1-luc reporter, 5×10^7 pfu RSV β -gal) were delivered to 8–10 week old male C57BL/6J-*Tyrc-2J/J*, C57BL/6J, B6.V-*lep*<ob>/J, B6.Cg-*m*+/*Lepr*<db>/J or diet-induced obesity (DIO) mice by tail vein injection. These mice were purchased from Jackson Labs (Bar Harbor, ME). All

mice were adapted to their environment for 1 week before study and were housed in colony cages with 12h light/dark cycle in a temperature-controlled environment. For in vivo imaging experiments, mice were imaged on day 3–5 after adenovirus delivery. Wild-type CRTC2, mutant Ser171Ala CRTC2, CRTC2 RNAi, unspecific RNAi, CRE-luc and RSV β -gal adenoviruses have been described previously 1. Ad-ATF6 α RNAi was constructed using the sequence: GGGAGTCAGACCTATGGAGCCC. Xbp1-luc was made from mouse Xbp1 promoter region spanning from –614 to –1.

In vivo imaging

Mice were imaged as described 1 under ad libitum feeding conditions or after fasting for 6 hours. Fasted mice were injected intraperitoneally (IP) with glucagon (100 mg/kg, Sigma), tunicamycin (TUN, 1 g/kg, Calbiochem) 6, or vehicle. Prior to imaging, mice were injected IP with 50 mg/kg Nembutal (Abbott Laboratories) and 100 mg/kg sterile firefly D-luciferin (Biosynth AG). Mice were imaged on the IVIS 100 Imaging System, and analyzed with Living Image software (Xenogen) 1 hour following glucagon injection and 10 hours after TUN administration.

In vivo analysis

Mouse tissues were sonicated, centrifuged and supernatants were reserved for β -gal activity, protein determinations, and SDS–PAGE analysis. Blood glucose values were determined using a LifeScan automatic glucometer. Glucose tolerance tests were performed by glucose IP administration (1 g/kg) after overnight fasting on day 5 after injection with Ad-GFP or Ad-ATF6N adenovirus.

Cell culture and fractionation

Mouse CRL-2189 (ATCC) cells were cultured in DMEM. Mouse primary hepatocytes were isolated and cultured as previously described 1. For reporter studies, Ad-CRE-Luc or Ad-Xbp1-luc infected hepatocytes (1 pfu per cell) were exposed to forskolin (FSK, 10 μ M) for 4h, or thapsigargin (THA, 5 μ g/ml) or tunicamycin (TUN, 200 nM) for 12–15h. For cyclosporine A (CsA, 5 μ M) inhibition, hepatocytes were pretreated with CsA for 1–2h. For double stimulation with FSK and THA, or FSK and TUN, hepatocytes were pretreated with THA or TUN for 4h, and then co-incubated with FSK for another 4h. Glucose output from primary hepatocytes was determined enzymatically, following 1 h collection in glucose-free M199 media supplemented with 10 mM lactate and 1 mM pyruvate 12. Cellular fractionation was performed as reported 18.

Immunoblot, immunoprecipitation, GST pull-down, and immunostaining

Immunoblot, immunoprecipitation, GST pull-down and immunostaining assays were performed as described 12. CRTC2, pCREB and CREB antibodies were previously described 2. The antibody anti-ATF6 α was purchased from IMGENEX, anti-tubulin from Upstate, anti-HA from Covance, anti-EEA1 from BD Pharmingen, anti-KDEL, GRP94 and TGN46 from Abcam, anti-Xbp1, JNK, cytochrome C from Santa Cruz, and anti-pJNK, pEIF2 α , eIF2 α , pAKT, AKT, pIRS1, IRS1 from Cell Signaling.

Chromatin immunoprecipitation and quantitative PCR

Chromatin immunoprecipitation (ChIP) assays were performed as previously described 2. The primers for G6Pase (5'GGAGGGCAGCCTCTAGCACTGTCAA3', 5'TCAGTCTGTAGGTCAATCCAGCCCT3') and Xbp1(5'GGCCCAGTTTGCACGGCGGAGAACA3', 5'CACCGCCCCGTGGCCTCCTGCCGC3') were used for ChIP analysis. All signals were normalized to the input chromatin signals. Total cellular RNAs from whole liver or from primary hepatocytes were extracted using the RNeasy kit (Qiagen). mRNA levels were measured as previously described 1.

Mass spectrometry

Immunoprecipitates of endogenous and HA-tagged CRTC2 from HEK293T were prepared for Mass Spectrometric studies as previously reported 12 and analyzed by electrospray ionization tandem mass spectrometry on a Thermo LTQ Orbitrap instrument.

Statistical analyses

All studies were performed on at least 3 independent occasions. Results are reported as mean \pm s.e.m. The comparison of different groups was carried out using two-tailed unpaired Student's *t*-test. Differences were considered statistically significant at $P < 0.05$.

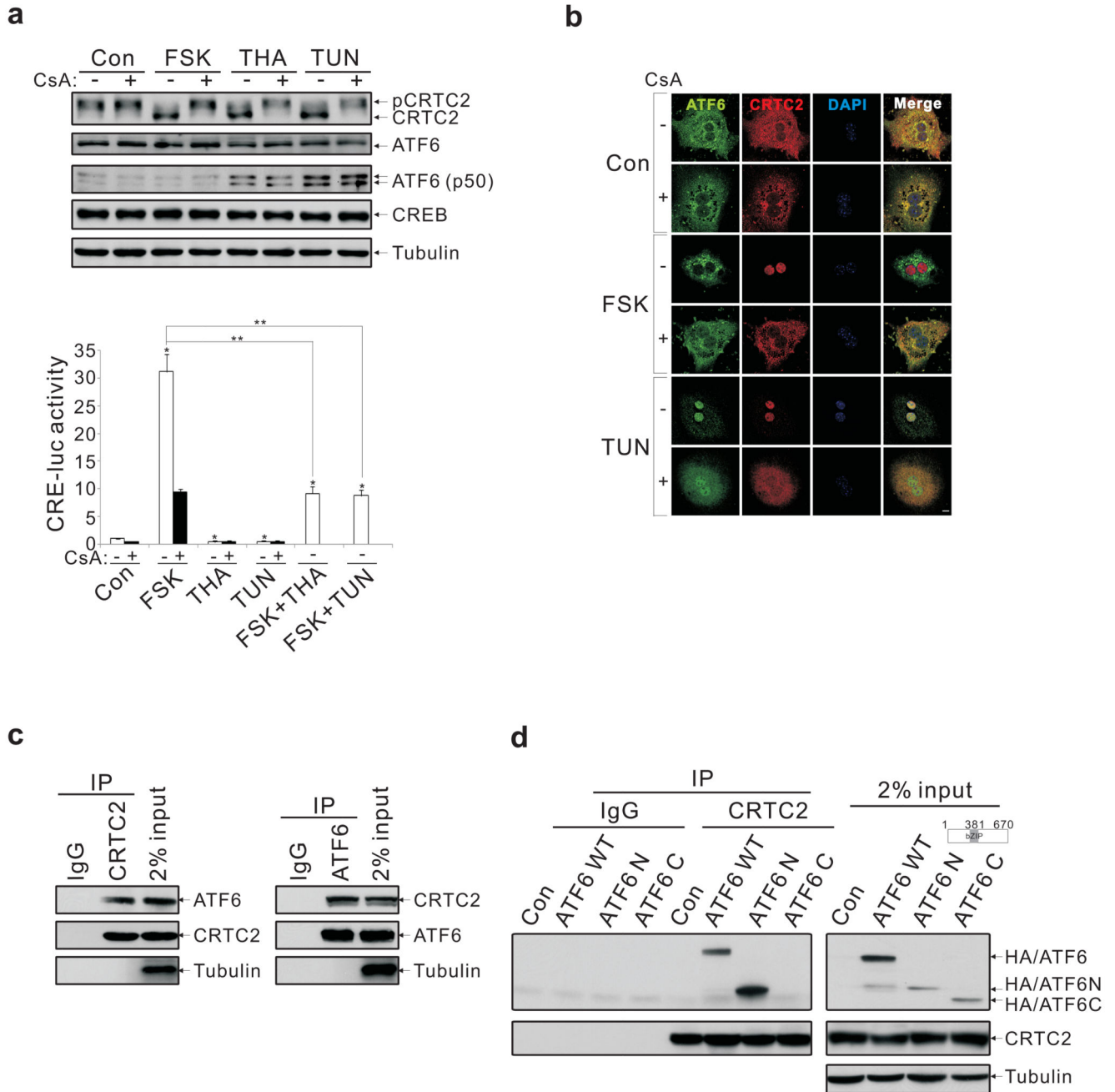
ACKNOWLEDGEMENTS

This work was supported by grants from the NIH, by the Clayton Foundation for Medical Research, and by the Keickhefer Foundation. We thank Nina Miller, Susan Hedrick, and Yi Liu for technical assistance and helpful discussions.

REFERENCES

1. Dentin R, et al. Insulin modulates gluconeogenesis by inhibition of the coactivator TORC2. *Nature*. 2007; 449:366–369. [PubMed: 17805301]
2. Koo SH, et al. The CREB coactivator TORC2 is a key regulator of fasting glucose metabolism. *Nature*. 2005; 437:1109–1111. [PubMed: 16148943]
3. Ozcan U, et al. Endoplasmic reticulum stress links obesity, insulin action, and type 2 diabetes. *Science*. 2004; 306:457–461. [PubMed: 15486293]
4. Haze K, Yoshida H, Yanagi H, Yura T, Mori K. Mammalian transcription factor ATF6 is synthesized as a transmembrane protein and activated by proteolysis in response to endoplasmic reticulum stress. *Mol Biol Cell*. 1999; 10:3787–3799. [PubMed: 10564271]
5. Adachi Y, et al. ATF6 is a transcription factor specializing in the regulation of quality control proteins in the endoplasmic reticulum. *Cell Struct Funct*. 2008; 33:75–89. [PubMed: 18360008]
6. Wu J, et al. ATF6alpha optimizes long-term endoplasmic reticulum function to protect cells from chronic stress. *Dev Cell*. 2007; 13:351–364. [PubMed: 17765679]
7. Yoshida H, Matsui T, Yamamoto A, Okada T, Mori K. XBP1 mRNA is induced by ATF6 and spliced by IRE1 in response to ER stress to produce a highly active transcription factor. *Cell*. 2001; 107:881–891. [PubMed: 11779464]
8. Lin JH, et al. IRE1 signaling affects cell fate during the unfolded protein response. *Science*. 2007; 318:944–949. [PubMed: 17991856]
9. Yamamoto K, et al. Transcriptional induction of mammalian ER quality control proteins is mediated by single or combined action of ATF6alpha and XBP1. *Dev Cell*. 2007; 13:365–376. [PubMed: 17765680]

10. Kahn BB, Flier JS. Obesity and insulin resistance. *J Clin Invest*. 2000; 106:473–481. [PubMed: 10953022]
11. Saltiel AR. New perspectives into the molecular pathogenesis and treatment of type 2 diabetes. *Cell*. 2001; 104:517–529. [PubMed: 11239409]
12. Srecon RA, et al. The CREB coactivator TORC2 functions as a calcium- and cAMP-sensitive coincidence detector. *Cell*. 2004; 119:61–74. [PubMed: 15454081]
13. Bittinger MA, et al. Activation of cAMP response element-mediated gene expression by regulated nuclear transport of TORC proteins. *Curr Biol*. 2004; 14:2156–2161. [PubMed: 15589160]
14. Yoshida H, et al. ATF6 activated by proteolysis binds in the presence of NF-Y (CBF) directly to the cis-acting element responsible for the mammalian unfolded protein response. *Mol Cell Biol*. 2000; 20:6755–6767. [PubMed: 10958673]
15. Iourgenko V, et al. Identification of a family of cAMP response element-binding protein coactivators by genome-scale functional analysis in mammalian cells. *Proc Natl Acad Sci U S A*. 2003; 100:12147–12152. [PubMed: 14506290]
16. Conkright MD, et al. TORCs: transducers of regulated CREB activity. *Mol Cell*. 2003; 12:413–423. [PubMed: 14536081]
17. Oyadomari S, Harding HP, Zhang Y, Oyadomari M, Ron D. Dephosphorylation of translation initiation factor 2 α enhances glucose tolerance and attenuates hepatosteatosis in mice. *Cell Metab*. 2008; 7:520–532. [PubMed: 18522833]
18. Robinson LJ, Pang S, Harris DS, Heuser J, James DE. Translocation of the glucose transporter (GLUT4) to the cell surface in permeabilized 3T3-L1 adipocytes: effects of ATP insulin, and GTP gamma S and localization of GLUT4 to clathrin lattices. *J Cell Biol*. 1992; 117:1181–1196. [PubMed: 1607382]

**Figure 1.**

Nuclear translocation and association of CRTc2 with ATF6 α in response to ER stress. A. Effects of ER stress activators (THA, TUN) and FSK on CRTc2 dephosphorylation (top) and Ad-CRE luc reporter activity (bottom) in primary hepatocytes. Pre-treatment with calcineurin inhibitor cyclosporine (CsA) indicated. Results are average of three independent experiments ($P^* < 0.01$; $P^{**} < 0.001$). B. Immunostaining for CRTc2 and ATF6 α in primary hepatocytes exposed to FSK or TUN. Scale bar; 5 μ m. C. Immunoblot showing co-immunoprecipitation (co-IP) of endogenous CRTc2 with ATF6 α in primary hepatocyte extracts. D. Immunoblot showing relative association of CRTc2 with transcriptionally

active ATF6 α N-terminal domain (aa. 1–381; ATF6 N) or C-terminal ER luminal domain (aa. 382–670; ATF6 C) by co-IP assay of transfected HEK293T cells.

Author Manuscript

Author Manuscript

Author Manuscript

Author Manuscript

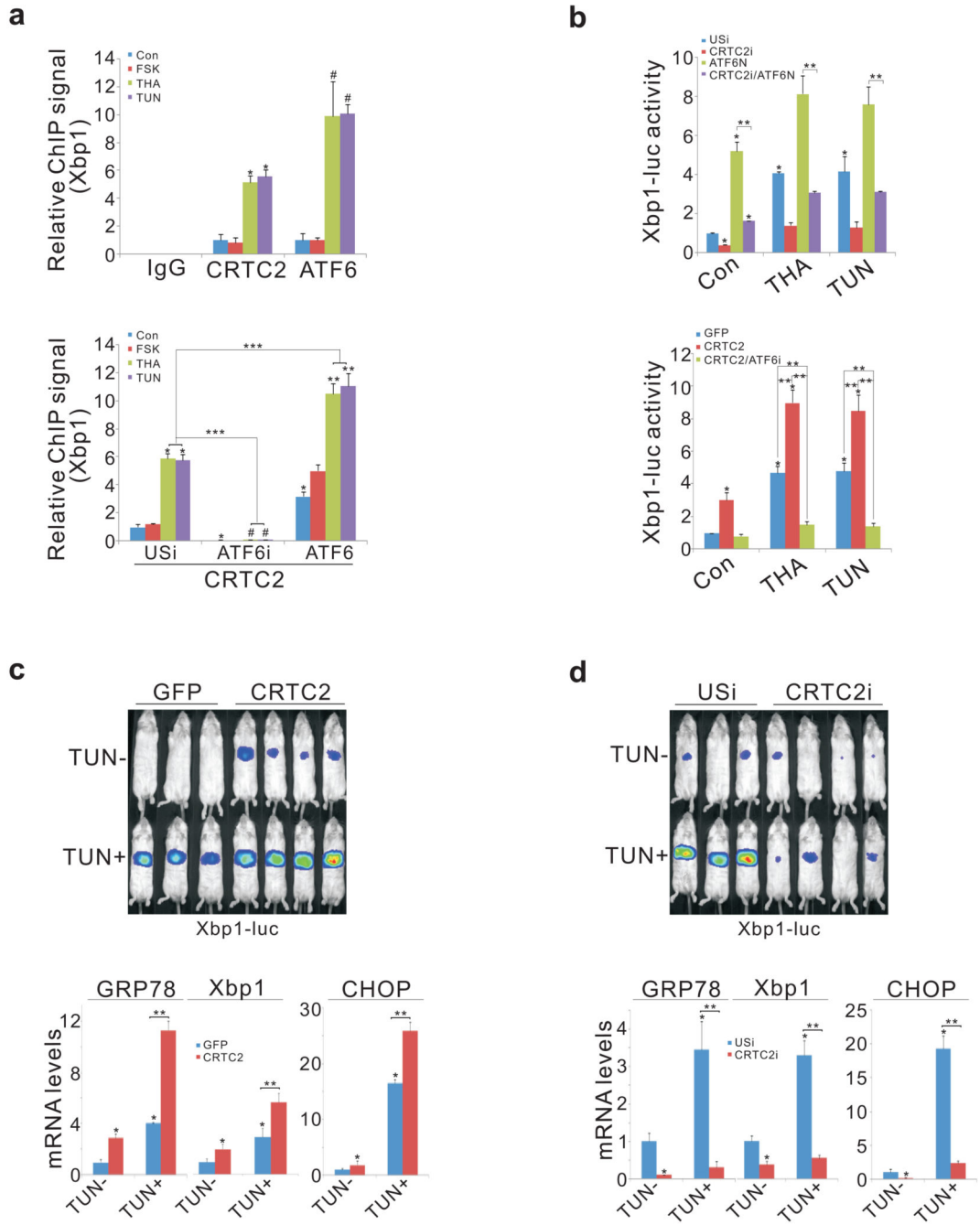


Figure 2. CRTC2 stimulates the expression of ER quality control genes through an association with ATF6 α . A. Top, chromatin immunoprecipitation (ChIP) assay showing occupancy of CRTC2 and ATF6 α over the Xbp1 promoter in primary hepatocytes exposed to THA or TUN. Bottom, effect of adenoviral ATF6 α over-expression or RNAi mediated knockdown (ATF6i) on CRTC2 occupancy. ($P^* < 0.01$; $P^\# < 0.01$; $P^{**} < 0.01$; $P^{***} < 0.001$; $n=3$) B. Top, effect of adenoviral ATF6N on Ad-Xbp1 luc reporter activity in control (USi) and CRTC2-depleted (CRTC2i) cells. Bottom, effect of Ad-CRTC2 on Ad-Xbp1 luc reporter

activity in control and ATF6 α -depleted hepatocytes. ($P^* < 0.01$; $P^{**} < 0.01$; $n=4$). C. and D. Top, hepatic Ad-Xbp1 luc reporter activity in mice injected intraperitoneally (IP) with TUN or vehicle. Effect of Ad-CRTC2 over-expression (C) or Ad-CRTC2 RNAi (D) on Ad-Xbp1 luc activity (top) and on hepatic mRNA amounts for ATF6 α -regulated genes ($P^* < 0.01$; $P^{**} < 0.01$; $n=4$).

Author Manuscript

Author Manuscript

Author Manuscript

Author Manuscript

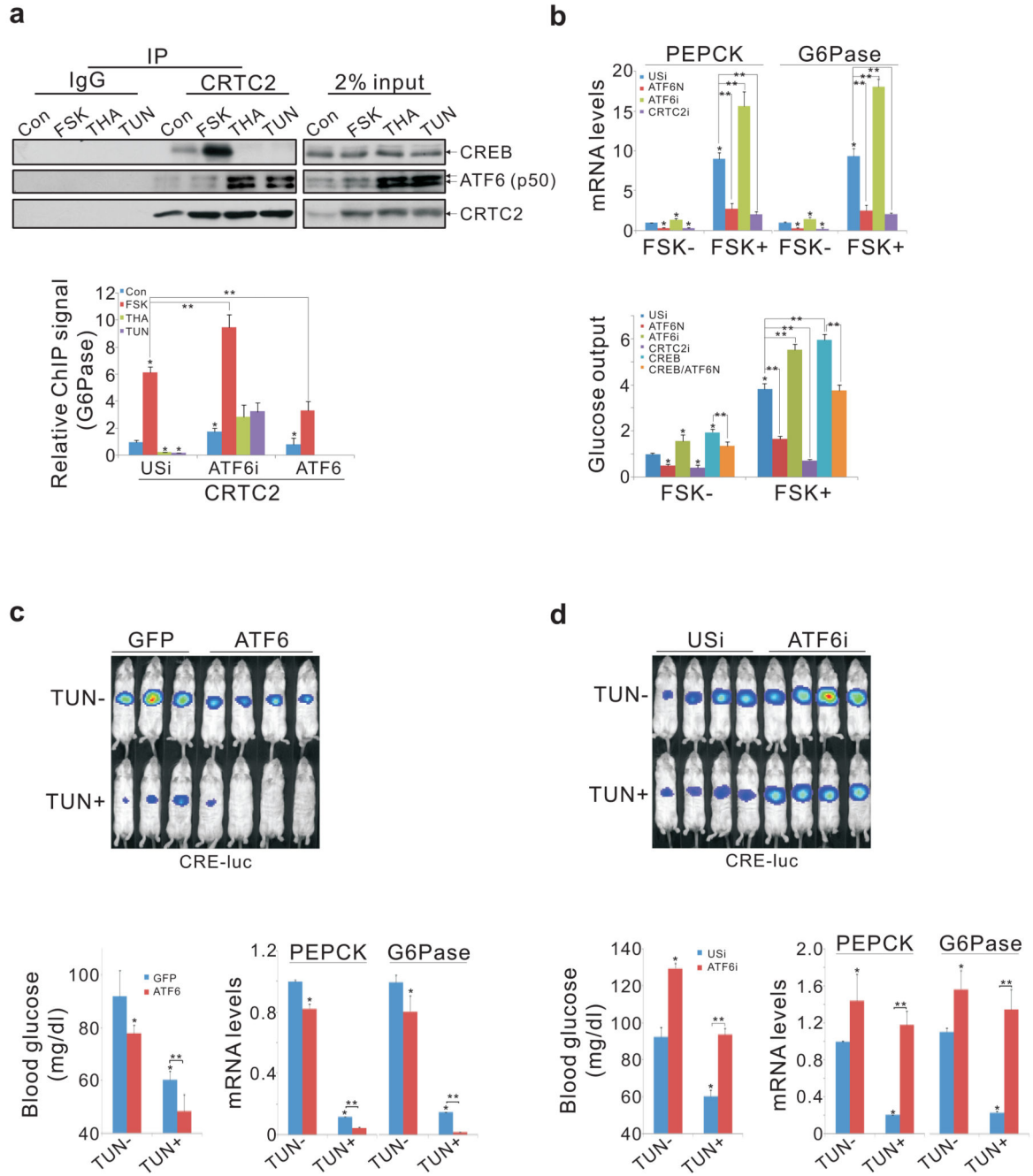


Figure 3.

CRTC2 mediates cross-talk between hepatic ER stress and fasting pathways. A. Top, immunoblot showing recovery of CREB from co-IPs of CRTC2 prepared from nuclear extracts of primary hepatocytes exposed to FSK, TUN, or THA. Bottom, effect of ATF6 α over-expression or RNAi-mediated depletion (ATF6i) on CRTC2 occupancy over the G6Pase promoter ($P^* < 0.01$; $P^{**} < 0.01$; $n=4$). B. Effect of ATF6 α over-expression or RNAi-mediated knockdown on gluconeogenic gene expression (top; $n=4$) and glucose secretion (bottom; $n=5$) in primary hepatocytes exposed to FSK. ($P^* < 0.01$ versus con; P^{**}

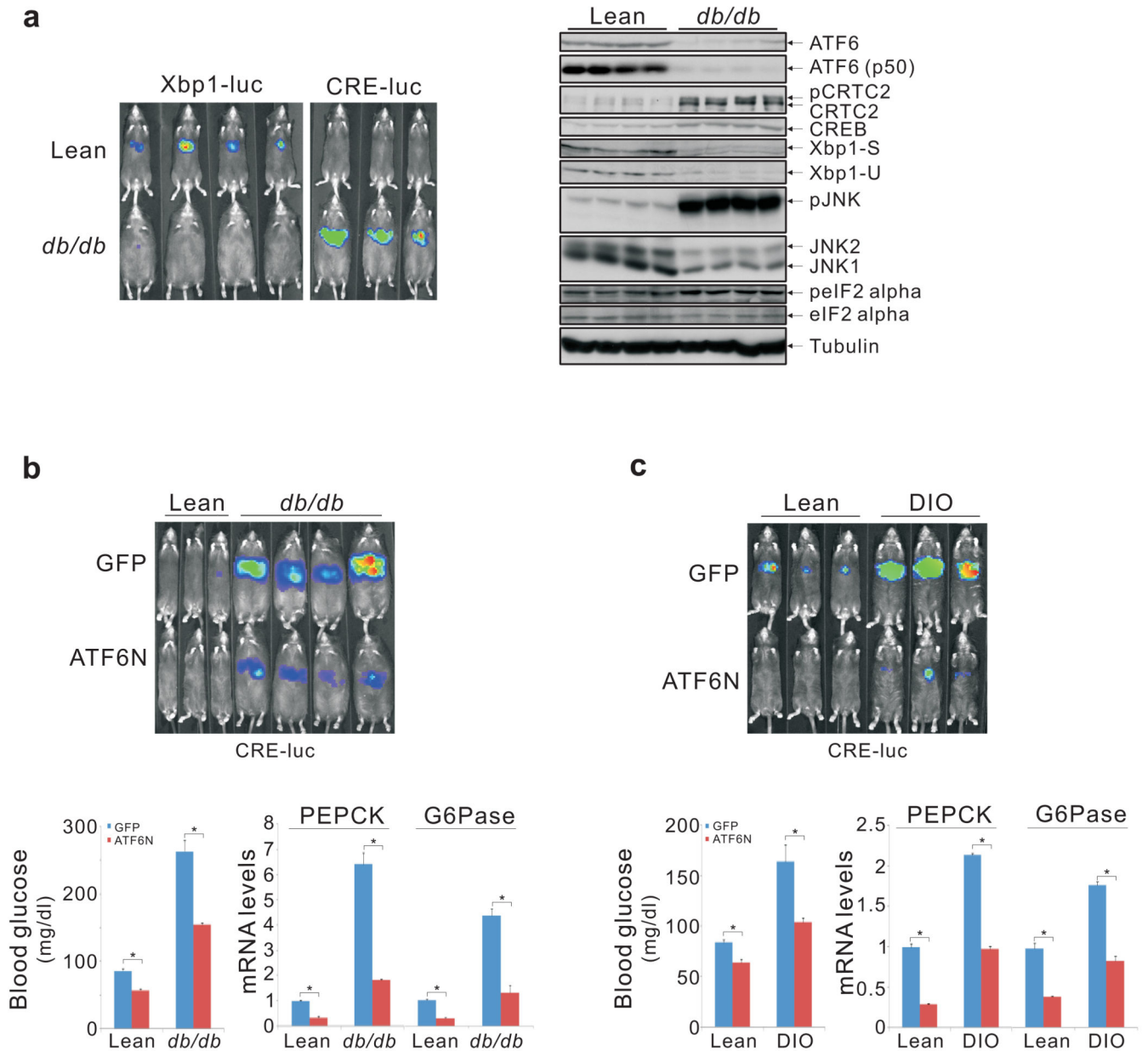
< 0.01). C. and D. Effect of ATF6 α over-expression (C) or RNAi-mediated depletion (D) on hepatic Ad-CRE luc activity (top), circulating blood glucose concentrations (bottom left), and gluconeogenic gene expression in fasted mice injected IP with TUN or vehicle ($P^* < 0.01$; $P^{**} < 0.01$; $n=4$).

Author Manuscript

Author Manuscript

Author Manuscript

Author Manuscript

**Figure 4.**

Reciprocal down-regulation of ATF6 α and up-regulation of CREB in obesity. A. Left, hepatic Ad-Xbp1 luc and Ad-CRE luc activities in obese *db/db* mice relative to lean controls. Right, immunoblot of hepatic extracts from wild-type and *db/db* mice showing protein amounts of ATF6 α and other ER stress markers. B. and C. Effect of Ad-ATF6N relative to Ad-GFP control on hepatic Ad-CRE luc activity (top), blood glucose concentrations (bottom left), and gluconeogenic gene expression (bottom right) in *db/db* (B) and high fat diet fed (DIO, C) mice compared to lean controls ($P^* < 0.01$; $n=4$).